Path integral Monte Carlo study of the internal quantum state dynamics of a generic model fluid

F. Schneider and P. Nielaba
Institut für Physik, Universität Mainz, KoMa 331, D-55099 Mainz, Germany
(Received 14 February 1996)

We study the quantum dynamics of a generic model fluid with internal quantum states and classical translational degrees of freedom in two spatial dimensions. The path integral Monte Carlo data for the imaginary time correlation functions are presented and analyzed by the maximum entropy method. A comparison of the frequency distribution with those of a mean field approximation and virial expansion shows good agreement at high and low densities, respectively. [S1063-651X(96)15211-9]

PACS number(s): 61.20.Ja, 05.30.−d, 02.70.Lq, 64.60.Cn

The computer simulation of models for condensed matter systems has become an important investigative tool in both fundamental and engineering research [1]. For the realistic modeling of real materials at low temperatures it is essential to take quantum degrees of freedom into account. Although big progress has been achieved on this topic [2,3], computer simulation of quantum systems still lags behind the development in the field of classical systems. This holds particularly for the determination of dynamical information, which was not possible until recently [4–6].

Now a successful method to obtain dynamical information from computer simulations of quantum systems has recently been proposed by Gubernatis and co-workers [4]. It uses concepts from probability theory and Bayesian logic to solve the analytic continuation problem to obtain real time dynamical information from imaginary time computer simulation data. The method has become known under the name *maximum entropy* (MaxEnt), and has a wide range of applications in other fields apart from physics.

Recently, phase transitions in two-dimensional systems [7] have received much attention in experimental [8] as well as in Monte Carlo (MC) [9–12] studies of adsorbed layers, in particular at low temperatures where quantum effects become important. In this paper we report some results on the dynamics of the internal quantum state of a generic two-dimensional model fluid. The model [13–15,10,11] is intended to mimic an adsorbate in the limit of strong binding and small corrugation. No attempt is made to model any real adsorbate realistically. Despite the crudeness of the model, it has been shown by various previous investigations [10,11] that it captures the essential features also observed in real adsorbates. For example, the quite complex phase diagram of the model is in qualitative agreement with that of real substances. While the previous investigations of the model focused on static properties, in this paper we present a study of the real time quantum dynamics, which can be considered as a prototype study of the dynamics of a quantum degree of freedom of an interacting many particle system in continuum.

The model Hamiltonian of the system is given by

$$H=\sum_{i=1}^{N}\frac{\mathbf{p}_i^2}{2M}-\frac{\omega_0}{2}\sum_{i=1}^{N}\sigma_i^x+\sum_{i<j}U(r_{ij})-\sum_{i<j}J(r_{ij})\sigma_i^z\sigma_j^z, \tag{1}$$

where M is the particle mass, $\mathbf{p}_i$ is the momentum of particle i, r_{ij} is the distance between particles i and j, and σ^x and σ^z are the usual Pauli spin half-matrices, $\hbar=1$. The potential energy consists of a one-particle (two-level) part with tunnel splitting ω_0 and two pair interaction terms $U(r)$ and $J(r)$. We chose $U(r)$ to be a hard disk potential for particles with diameter d and $J(r)$ to be a square well potential with $J(r)=J$ for $d<r<1.5d$ and zero elsewhere. The crucial coupling between quantum and classical variables is achieved via the distance dependence of the interaction $J(r)$ between the internal quantum states. The total number of particles N and the total volume V is fixed; the dimensionless density is $\rho^*=\rho d^2=Nd^2/V$. The particles are constrained to move in two spatial dimensions. In the adiabatic approximation we assume a separation of time scales for the translational and internal degrees of freedom and treat the translations classically, which is justified for large particle masses M. This approximation does indeed hold for a variety of adsorbates. Thus the Hamiltonian contains both quantum and classical degrees of freedom. The quantum degrees of freedom are treated using path integral Monte Carlo (PIMC) techniques. This yields dynamical correlations functions in imaginary time which are then converted to real frequency spectral densities using the maximum entropy method.

Application of the Trotter formula [3] results in the following expression for the system's partition function $Z(\beta,N,V)=\lim_{P\to\infty}Z_P(\beta,N,V)$ at temperature $T^*=(\beta J)^{-1}$, with the discretized partition function [14,15,10,11] for fixed Trotter dimension P being

$$Z_P(\beta,N,V)=\frac{A_P^{NP}}{\lambda^{2N}N!}\int d\mathbf{r}^N\exp\left[-\beta\sum_{i<j}U(r_{ij})\right]\times\sum_{\{S\}}\exp[-\beta\{W_{\mathrm{eff}}^{\mathrm{x}}(\{S\})+W_{\mathrm{eff}}^{\mathrm{z}}(\{S\},\{r\})\}]. \tag{2}$$

$W_{\mathrm{eff}}^{\mathrm{x}}(\{S\})=-\Sigma_{i=1}^{N}\Sigma_{p=1}^{P}K_P S_{i,p}S_{i,p+1}$ denotes the effective *intramolecular* potential and $W_{\mathrm{eff}}^{\mathrm{z}}(\{S\},\{r\})=-(1/P)\Sigma_{i<j}^{N}\Sigma_{p=1}^{P}J(r_{ij})S_{i,p}S_{j,p}$ the effective *intermolecular* potential, with the pseudospin variables $S_{i,p}=\pm1$, $A_P=[\frac{1}{2}\sinh(\beta\omega_0/P)]^{1/2}$ and $K_P=(1/2\beta)\ln[\coth(\beta\omega_0/2P)]$.

λ denotes the thermal de Broglie wavelength and the quantum chains have to satisfy periodic boundary conditions with respect to P.

The equivalent classical Hamiltonian resulting from this expression for the partition function was then used in canonical Metropolis Monte Carlo simulations. We denote thermal averages of an observable $\mathcal{A}$ as $\langle \mathcal{A} \rangle$. The simulations were performed for $\omega^* = \omega_0 / J = 4$ (where $J = 1$) with $N = 256$ particles and a Trotter dimension $P = 64$ chosen to achieve good computer performance. Since a value for P satisfying $P/\beta J \approx 40$ was found to be sufficient for convergence to the quantum limit [10], at temperature $T^* = 1$ the chosen value of P was larger than necessary. Since it is well known that noise works through in a very nonlinear way on the MaxEnt results we tested our implementation of the procedure by adding relative Gaussian noise with a standard deviation of 0.8% on correlation function data in the low density limit. The shape and position of the MaxEnt frequency distribution (see below) is qualitatively maintained, but the width of the distribution is increased by a factor of about 1.5. It turned out that only data with noise of less than 0.1% lead to statistically reliable results which were only possible to obtain with about 10^7 MC steps. The whole study took approximately 5000 CPU hours on a CRAY YMP. Standard particle displacements were performed as well as spin flips. One MC step consisted of 256 attempted translational displacements and spin flip attempts of chain segments randomly varying in length from 1 to P so that 64 spins were attempted to be flipped in one MC step.

The system has a rich phase diagram [10,11] and in particular a phase transition from a paramagnetic fluid phase at low densities to a ferromagnetic fluid phase at high densities for temperatures above the tricritical point (at $T^* \approx 0.55$). Here the magnetization m_i of particle i is defined as the average of the ''classical spins'' along the Trotter chain, $m_i = \langle \Sigma_{p=1}{}^P S_{i,p} \rangle / P$. In the paramagnetic region of the phase diagram the dynamics of the internal degrees of freedom is quite different from the dynamics in the ferromagnetic region since in the latter the ''classical spins'' along the Trotter direction are pointing mainly in the same direction (high ''tunneling'' frequency) whereas in the paramagnetic region fluctuations of the spin values along the Trotter direction are frequent (low ''tunneling'' frequency). The dynamics near the continuous phase transition is of particular interest since at this point the correlation length diverges and the magnetic ordering differs in spatial regions of different sizes. This results in a mixing of the dynamics of low density paramagnetic areas with the dynamics of high density ferromagnetic areas, and thus the full dynamics should contain contributions from many ''tunneling'' frequency ranges; see below. In order to study the quantum dynamics of our adsorbate in the different regions of the phase diagram in detail with the methods mentioned above, we focused on a particular choice of the temperature, $T^* = 1$. The imaginary time correlation functions $\mathcal{G}(\tau) = \langle \sigma^z(\tau) \sigma^z(0) \rangle$ of the σ^z-spins are given by

$$\mathcal{G}(\tau) = \frac{1}{N} \sum_{i=1}^{N} \langle e^{\tau H} \sigma_i^z e^{-\tau H} \sigma_i^z \rangle \tag{3}$$

with $0 \leq \tau \leq \beta$. The numerical values $G(\tau)$ at imaginary time $\tau = p\beta/P$ $(p = 1,2, \ldots, P)$ are obtained from

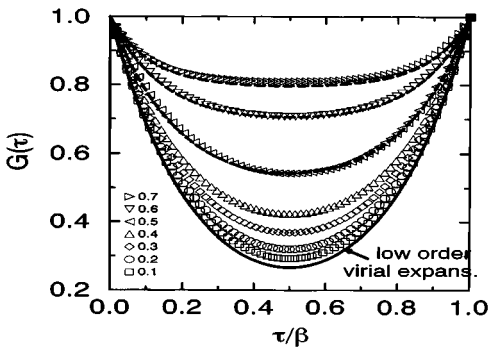

FIG. 1. PIMC results (symbols) of the σ^z imaginary time correlations $G(\tau)$ versus imaginary time for the densities $\rho^* = 0.1, 0.2, \ldots, 0.7$ from bottom to top, the temperature is $T^* = 1$. The full line shows the results for $\mathcal{G}(\tau)$ according to the lowest order virial expansion, the dashed lines give the MF values of $\mathcal{G}(\tau)$ for the densities $\rho^* = 0.7, 0.6$ and 0.5 from top to bottom.

$$G(p\beta/P) = \frac{1}{NP} \left\langle \sum_{i=1}^{N} \sum_{p=1}^{P} S_{i,p} S_{i,p+1} \right\rangle. \tag{4}$$

The first term of a virial expansion [15] of the correlation function is

$$\mathcal{G}(\tau) = \frac{\cosh[\omega_0(\tau - \beta/2)]}{\cosh[\omega_0 \beta/2]}. \tag{5}$$

It represents the correlations of noninteracting particles.

In mean field approximation we obtain for the imaginary time correlation functions [15]

$$\mathcal{G}(\tau) = J_0^2 m^2 / (\Omega/2)^2 + (\omega_0/\Omega)^2 \frac{\cosh[\Omega(\tau - \beta/2)]}{\cosh[\Omega\beta/2]}, \tag{6}$$

where $J_0 = \rho \int d^2 r J(r) g(r)$ is determined by the classical correlation function $g(r)$, which was computed iteratively in Percus-Yevick approximation in two spatial dimensions. $\Omega/2 = [(J_0 m)^2 + (\omega_0/2)^2]^{1/2}$, and the magnetization m is solution of the equation

$$m(h) = \frac{J_0 m(h) + h}{\Omega(h)/2} \tanh[\beta \Omega(h)/2] \tag{7}$$

for $h \to 0$. From Eq. (6) we see that for $m \neq 0$ the mean field–correlation function contains a time independent constant $J_0^2 m^2 / (\Omega/2)^2$, which leads to a peak at $\omega = 0$ in the spectral density; see below.

The PIMC data obtained for the imaginary time correlations are shown in Fig. 1 for different densities at $T^* = 1$. The relative errors of the data are of the order 10^{-4}, which is necessary for the maximum entropy method to work when there is little previous knowledge as in the present case. At low densities the average particle distances are large and since the particle interaction is restricted to a ''square well'' region $[d < r < 1.5d$, see Eq. (1)], the probability for particle interactions is small. Thus the particles occupy mainly σ^x eigenstates resulting in a small correlation of the σ^z spins and a small value of $G(\beta/2)$. In the limit of zero density the dynamics is purely given by the tunneling of the spins with

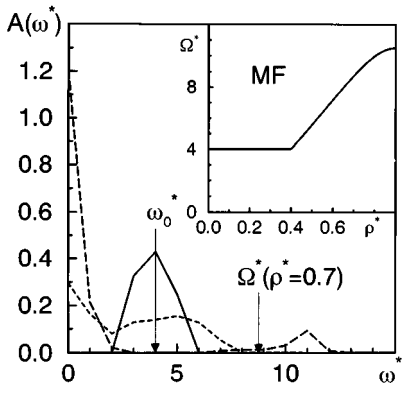

FIG. 2. $A(\omega)$ via MaxEnt for the densities (a) $\rho^*=0.1$ (full line), (b) $\rho^*=0.45$ (dashed line), (c) $\rho^*=0.7$ (long dashed line), the temperature is $T^*=1$, in all cases a flat default model in the maximum entropy procedure was used. The vertical lines refer to the results of the mean field approximation for $\Omega^*=\Omega/J=\omega_0^*$ for $\rho^*=0.1$ and $\Omega^*(\rho^*=0.7)$. Inset: Mean field frequency $\Omega^*=\Omega/J$ versus density at temperature $T^*=1$.

frequency ω_0 which can be described by the zeroth order term in the virial expansion [15] [see Eq. (5)], which is shown in Fig. 1 for comparison. At higher densities the probability for interaction increases and the particles ''hybridize'' by leaving their σ^x ground states and occupying more and more σ^z eigenstates and thus the value of $G(\beta/2)$ increases. This effect finally even leads to a continuous phase transition [10] from a paramagnetic to a ferromagnetic phase at about $\rho_c^*\approx 0.53$. In mean field approximation [15] the critical density is at $\rho_{c,MF}^*=0.4$, and from Eq. (6) we see that for all $\rho^*<\rho_{c,MF}^*$ the resulting correlation functions agree with the lowest order virial expansion result, since the mean field (MF) value for m is zero. Thus the MF correlation functions increasingly deviate from the PIMC data with increasing density. Only for $\rho^*>\rho_{c,MF}^*$ there is reasonably good agreement.

In the inset of Fig. 2 we show the mean field frequency $\Omega^*=\Omega/J$ as a function of density for $T^*=1$. At this temperature the system undergoes a phase transition from a paramagnetic to a ferromagnetic fluid at a density whose mean field value is $\rho_{c,MF}^*=0.4$. For densities below this value we obtain $\Omega=\omega_0$, which agrees with the frequency value of the low order virial expansion; see Eq. (5). For $\rho>\rho_{c,MF}$, Ω increases with the density due to increase of the magnetization.

Besides the deviation mentioned above the main problem of the dynamical information from the MF approximation is that it contains only one positive frequency and so the resulting real time correlations cannot be damped or describe localizations ''on one side of the double well'' due to interference effects as one expects for real materials. Thus we expect that the frequency distribution is not singly peaked but has a broad distribution, perhaps with several maxima instead of a single peak at an average mean field frequency. In order to study the shape of the frequency distribution we analyze the imaginary time correlations in more detail.

We briefly repeat now the essential parts of the *maximum entropy* method, for details we refer to the literature [4]. We seek to obtain information on the dynamics of the internal degree of freedom of the model from PIMC simulations. The solution of this problem is not straight forward, since PIMC simulations yield dynamical correlation functions in imaginary time whereas physically relevant, especially regarding comparison with experimental results, are of course real time data. Fortunately there is an integral relation,

$$\mathcal{G}(\tau)=\int_{-\infty}^{+\infty} d\omega \frac{e^{-\tau\omega}A(\omega)}{1\pm e^{-\beta\omega}}, \tag{8}$$

that connects correlations $\mathcal{G}(\tau)$ in imaginary time τ with real frequency spectral densities $A(\omega)$. If this relation could be inverted and if A could be determined from the numerical estimate $G(\tau)$ for $\mathcal{G}(\tau)$, one would have the desired dynamical information.

The double sign in Eq. (8) usually refers to Fermi– $(+)$ and Bose statistics $(-)$ respectively. In our system we neglect the statistics and study the σ^z ''self correlations.'' We consider the symmetrized correlation functions [16] resulting in the ''+'' sign in Eq. (8) and $A(\omega)=A(-\omega)$.

Since the numerical estimate $G(\tau)$ is necessarily incomplete and inaccurate the inversion is not possible without any ambiguity. Gubernatis and co-workers now suggested to resolve the ambiguity by choosing the most probable A consistent with the data G, i.e., they chose the A that maximizes the conditional probability $P[A|G]$. This is justified since A has the properties of a probability distribution function: $A(\omega)\geqslant 0$, $\int d\omega A(\omega)<\infty$, $A(\omega)$ is bounded.

The *a posteriori* probability $P[A|G]$ for having the spectral density $A(\omega)$ given the simulation data G is

$$P[A|G]\propto e^{Q} \tag{9}$$

with $Q=\alpha S-\chi^2/2$. S has the meaning of an entropy and is of the form

$$S=-\int d\omega\left(A(\omega)\ln\left[\frac{A(\omega)}{M(\omega)}\right]-A(\omega)+M(\omega)\right). \tag{10}$$

$M(\omega)$ is the *default model*, by which additional knowledge about system properties can be incorporated. Minimum additional knowledge is equivalent to $M(\omega)=\text{const}$. Without data, S is maximized by $A(\omega)=M(\omega)$. χ^2 measures the deviation of the time correlation function $\mathcal{G}$ computed from a proposed A via Eq. (8) from the PIMC value G at the point τ_k in imaginary time,

$$\chi^2=\sum_k [G(\tau_k)-\mathcal{G}(\tau_k)]^2/\sigma_k^2. \tag{11}$$

σ_k is the standard deviation of the simulation data for $G(\tau_k)$ at τ_k. The problem of maximizing $P[A|G]$ can be solved by maximizing Q with respect to $A(\omega)$, which is solved iteratively for given PIMC data for G.

In Fig. 2 we show $A(\omega)$ for the densities $\rho^*=0.1,0.45$ and 0.7. Due to results of virial expansions we expect that at low densities the behavior is dominated by the dynamics of the isolated particles, resulting in a peak in $A(\omega)$ at the tunneling frequency ω_0. With increasing density due to increasing probability of particle interactions we expect a broadening of the spectral density around ω_0. These expectations

have indeed been obtained by MaxEnt. In case of high densities where the system is in the ferromagnetic phase we obtain a double peak structure for $A(\omega)$ with a sharp peak at $\omega=0$ and a broadened peak at a higher frequency. The center of this peak is shifted to higher frequencies with increasing density. This behavior is plausible according to the mean field results which predict a peak at $\omega=0$ and a second peak at the frequcncy Ω. The values of Ω are close to the center of mass of the broadened high frequency peaks, see Fig. 2 for results at the density $\rho^*=0.7$.

For densities close to the phase transition density we obtain a broad frequency distribution, see Fig. 2. This shows that due to the diverging correlation length particles interact in spatial areas of different sizes, densities and magnetizations resulting in a spectral density approximatively being given as a superposition of the functions corresponding to the ferromagnetic and paramagnetic cases. In this region of the phase diagram the results of the mean field study are not reliable, since critical fluctuations are not treated properly in this approximation. In order to analyze the quantum dynamics of a two-dimensional fluid undergoing a phase transition it turns out to be essential to go beyond MF approximation and to apply methods as those presented in this paper.

F.S. thanks the Deutsche Forschungsgemeinschaft DFG for the support (Grant No. Ni-259/6-2) and P.N. thanks the DFG for support (Heisenberg Foundation). The computations were carried out on the CRAY-YMP of the HLRZ at Jülich and of the RHRK at Kaiserslautern.

[1] *Applications of the Monte Carlo Method in Statistical Physics*, edited by K. Binder (Springer, Berlin, 1984); M.P. Allen and D.J. Tildesley, *Computer Simulation of Liquids* (Clarendon Press, Oxford, 1987).

[2] J.A. Barker, J. Chem. Phys. **70**, 2914 (1979); D. Chandler and P.G. Wolynes, *ibid.* **74**, 4078 (1981).

[3] B.J. Berne and D. Thirumalai, Annu. Rev. Phys. Chem. **37**, 401 (1986); *Quantum Simulation of Condensed Matter Phenomena*, edited by J.D. Doll and J.E. Gubernatis (World Scientific, Singapore, 1990); K.E . Schmidt and D.M. Ceperley, in *The Monte Carlo Method in Condensed Matter Physics*, Topics in Applied Physics Vol. 71, edited by K. Binder (Springer, Berlin, 1992).

[4] J.E. Gubernatis, M. Jarrell, R.N. Silver, and D.S. Sivia, Phys. Rev. B **44**, 6011 (1991); R.N. Silver, D.S. Sivia, J.E. Gubernatis, *ibid.* **41**, 2380 (1990); M. Jarrell and J.E. Gubernatis (unpublished).

[5] E. Gallicchio and B. Berne, J. Chem. Phys. **101**, 9909 (1994).

[6] C.H. Mak and D. Chandler, Phys. Rev. A **41**, 5709 (1990).

[7] *Phase Transitions in Surface Films 2*, edited by H. Taub, G. Torzo, H.J. Lauter, and S.C. Fain, Jr. (Plenum, New York, 1991).

[8] H. Wiechert and S.-A. Arlt, Phys. Rev. Lett. **71**, 2090 (1993).

[9] O. Opitz, D. Marx, S. Sengupta, P. Nielaba, and K. Binder, Surf. Sci. Lett. **297**, L122 (1993); D. Marx, O. Opitz, P. Nielaba, and K. Binder, Phys. Rev. Lett. **70**, 2908 (1993); V. Pereyra, P. Nielaba, and K. Binder, J. Phys. Condens. Matter **5**, 6631 (1993); D. Marx, S. Sengupta, P. Nielaba, and K. Binder, Phys. Rev. Lett. **72**, 262 (1994).

[10] D. Marx, P. Nielaba, and K. Binder, Phys. Rev. Lett. **67**, 3124 (1991); Phys. Rev. B **47**, 7788 (1993); S. Sengupta, D. Marx, and P. Nielaba, Europhys. Lett. **20**, 383 (1992); A.C. Mitus, D. Marx, S. Sengupta, P. Nielaba, A.Z. Patashinskii, and H. Hahn, J. Phys. Condens. Matter **5**, 8509 (1993).

[11] F. Schneider, D. Marx, and P. Nielaba, Phys. Rev. E **51**, 5162 (1995); F. Schneider, M.O. Ihm, and P. Nielaba, in *Computer Simulation Studies in Condensed–Matter Physics VII*, edited by D.P. Landau, K.K. Mon, and H.B. Schüttler (Springer, Berlin, 1994), p. 188.

[12] S. Sengupta, D. Marx, P. Nielaba, and K. Binder, Phys. Rev. E **49**, 1468 (1994).

[13] R.M. Stratt, J. Chem. Phys. **80**, 5764 (1984); S.G. Desjardins and R.M. Stratt, *ibid.* **81**, 6232 (1984).

[14] P. Ballone, P. de Smedt, J.L. Lebowitz, J. Talbot, and E. Waisman, Phys. Rev. A **35**, 942 (1987).

[15] P. de Smedt, P. Nielaba, J.L. Lebowitz, J. Talbot, and L. Dooms, Phys. Rev. A **38**, 1381 (1988).

[16] R. Kubo, M. Toda, and N. Hashitsume, *Statistical Physics II* (Springer, Berlin, 1985).